Optics Letters

Generation of axially modulated plasma waveguides using a spatial light modulator

G. A. Hine,* A. J. Goers, L. Feder, J. A. Elle, S. J. Yoon, and H. M. Milchberg

Institute for Research in Electronics and Applied Physics, University of Maryland, College Park, Maryland 20742, USA
**Corresponding author: ghine@umd.edu*

Received 18 May 2016; revised 22 June 2016; accepted 25 June 2016; posted 27 June 2016 (Doc. ID 266511); published 19 July 2016

We demonstrate the generation of axially modulated plasma waveguides using spatially patterned high-energy laser pulses. A spatial light modulator (SLM) imposes transverse phase front modulations on a low-energy (10 mJ) laser pulse which is interferometrically combined with a high-energy (130–450 mJ) pulse, sculpting its intensity profile. This enables dynamic and programmable shaping of the laser profile limited only by the resolution of the SLM and the intensity ratio of the two pulses. The plasma density profile formed by focusing the patterned pulse with an axicon lens is likewise dynamic and programmable. Centimeter-scale, axially modulated plasmas of varying shape and periodicity are demonstrated. © 2016 Optical Society of America

OCIS codes: (350.5400) Plasmas; (070.6120) Spatial light modulators.

http://dx.doi.org/10.1364/OL.41.003427

The extended high-intensity propagation of ultrashort laser pulses in gases and plasmas has been studied for applications including high harmonics [1], broadband coherent light generation and pulse shaping [2,3], laser amplification and pulse compression [4,5], high-power terahertz generation [6,7], guided electrical discharges [8,9], and charged particle acceleration [10,11]. Typically, high intensities are achieved by focusing laser pulses tightly. However, without linear or nonlinear focusing by the medium, this limits the interaction length to approximately the Rayleigh range. A waveguide can extend the interaction over many Rayleigh ranges, but it must be able to survive the guided fields. Plasma can be preformed into a guiding structure [12–14] which is able to withstand intensities many orders of magnitude higher than conventional optical materials. This is especially important for laser-driven acceleration schemes, including laser wakefield acceleration [15,16] and direct laser acceleration [11,17].

An elongated plasma with an on-axis density minimum has the refractive index profile of an optical guiding structure. One method to form such a structure, employed in this Letter, uses an axicon to focus an intense laser pulse to a line in clustered gases [13,18]. The resulting hot column of plasma expands at its ion acoustic speed, forming a shock wall as it propagates in the ambient gas. The plasma expansion results in a density profile with an on-axis minimum, which is suitable for optical guiding [16,19].

The clustered targets are formed by throttling high-pressure, cryogenically cooled gas out of a pulsed solenoid valve. The high-pressure gas cools as it expands into vacuum, and Van der Waals forces cause the molecules to coalesce into nanometer-scale solid density aggregates. These nanoclusters are efficient absorbers of high-intensity laser light [18], and it has been shown that clustered nitrogen can be used to produce uniformly ionized N^{5+} plasma waveguides when ionized with 100 ps laser pulses [16].

Even with a guiding structure present, many processes of interest are then limited by dephasing. As is well known for second-harmonic generation, a periodically poled nonlinear crystal or glass optical fiber can mitigate dephasing between the fundamental and second harmonic through quasi-phase matching [20]. Analogously, a periodic axial variation in a plasma guiding structure can be used to quasi-phase match either direct laser acceleration [11,17] or laser wakefield acceleration [21] of relativistic electrons.

In this Letter, we present a method for imposing programmable axial density variations on plasma waveguides. Axially modulated plasma waveguides have previously been demonstrated using two techniques. The first technique is to modulate the heating of a uniform elongated cluster jet by using a fixed transmissive "ring grating" to pattern the channel-forming pulse [17]. The second technique is to use an array of fine wires at the nozzle exit to corrugate the neutral atomic density. This is then ionized with a channel-forming Bessel beam (line focus), producing a modulated plasma waveguide [22]. Both methods offer deep modulations at periods down to 65 μm but produce only fixed structures. Since both the optimum modulation period and depth for quasi-phase matching depend on many experimental parameters [16,19], it is desirable to have a method to tune them *in situ*.

Here, we achieve heater modulations using a 2D spatial light modulator (SLM), which is an electro-optic liquid crystal array with a pixel-by-pixel-controllable linear birefringence. It is used to impose a transverse *phase modulation* on a low-energy laser pulse (10 mJ) that is interfered with a higher energy pulse (130–450 mJ), producing radial intensity modulations. The radially modulated beam is then focused through an axicon to generate a line focus with an axially modulated intensity.

The concept is shown schematically in Fig. 1. In prior work by another group [23], a 1D SLM and polarizer directly imposed *intensity modulations* on a high-power pulse which was then focused by a cylindrical lens, leading to axially modulated heating of a plasma channel. However, this method required sending over 100 mJ through the SLM and operating dangerously close to the liquid crystal damage threshold.

The use of interferometric beam combining for patterning the high-intensity pulse imposes a trade-off between efficient use of the laser energy and the achievable modulation depth. In order to investigate the relationship between modulation depth and efficiency, we write the field corresponding to the high-energy beam as $\mathbf{E}_1$ and that for the low-energy beam as $\mathbf{E}_2 = \epsilon \mathbf{E}_1 e^{i\Delta\varphi(\mathbf{r}_\perp)}$. Here, ϵ is the field amplitude splitting at the variable beam splitter, and $\Delta\varphi(\mathbf{r}_\perp)$ is the transverse phase shift profile imposed on the beam by the SLM. When initially divided, the split beams are orthogonally polarized, so a half-wave plate is used to rotate $\mathbf{E}_2$ parallel to $\mathbf{E}_1$, enabling interference at a nonpolarizing beam splitter of transmissivity T.

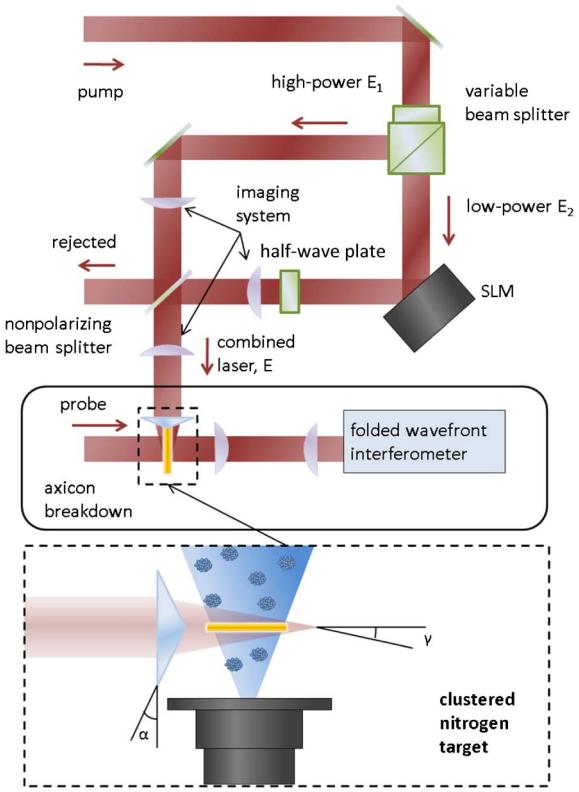

Fig. 1. Experimental setup. A variable polarizing beam splitter divides the input pump pulse into high-power ($\mathbf{E}_1$) and low-power ($\mathbf{E}_2$) pulses. The low-power pulse is patterned with a phase shift profile by a 2D reflective SLM, and its polarization is then rotated to match the high-power beam. The two arms are combined and interfered at a nonpolarizing beam splitter ($T = 0.75$) to produce transverse intensity modulations on the beam. The face of the SLM is imaged to a 28° base angle axicon. The high-power arm is imaged likewise. The axicon focuses the modulated beam to a line, causing axially modulated breakdown and heating. The plasma is probed by a synchronous 1064 nm, 140 ps pulse imaged into a folded wavefront interferometer.

The total field after combining at the beam splitter is

$$\mathbf{E} = \sqrt{T}\mathbf{E}_1 + \sqrt{1-T}e^{i\pi}\mathbf{E}_2 = (\sqrt{T} + \epsilon\sqrt{1-T}e^{i(\Delta\varphi+\pi)})\mathbf{E}_1, \quad (1)$$

leading to an intensity profile

$$I \propto |\mathbf{E}|^2 = (T - 2\epsilon\sqrt{T(1-T)}\cos(\Delta\varphi(\mathbf{r}_\perp)) + \epsilon^2(1-T))|\mathbf{E}_1|^2. \quad (2)$$

From Eq. (2), we determine a maximum possible modulation depth of

$$\Delta I/I_1 = 4\epsilon\sqrt{T(1-T)} \quad (3)$$

and maximum possible power throughput of

$$P_{\max}/P_1 = T + 2\epsilon\sqrt{T(1-T)} + \epsilon^2(1-T), \quad (4)$$

where P_1 is the power in the high-power arm.

The achievable total beam throughput and modulation depth each have global maxima with respect to the combining beam splitter transmissivity, T. As seen from Eq. (4), the maximum combined power occurs for $T_{P,\max} = 1/(\epsilon^2+1)$, with the associated modulation depth $(\Delta I/I_1)_{P,\max} = 4\epsilon^2/(\epsilon^2+1)$ and perfect efficiency $P_{\max}/P_1 = 1+\epsilon^2$. The maximum modulation depth, calculated from Eq. (3), occurs for $T = 0.5$, for which $(\Delta I/I_1)_{\max} = 2\epsilon$ and $P_{\max}/P_1 = 1/2(1+\epsilon)^2$. For the $T = 0.75$ combining beam splitter used in our experiments, $(\Delta I/I_1)_{\max} = 1.7\epsilon$. The advantage of our interferometric approach is that while the intensity modulation depth scales as ϵ, the power on the SLM stays at a safe level, scaling as ϵ^2. This enables extensive control of modulation depth while maintaining high laser power on target and low power at the SLM.

The transversely modulated pulse is then focused by an axicon to form an axially modulated Bessel beam. The modulated Bessel beam ionizes and heats the medium, and the intensity modulations result in an axially modulated plasma. The period of the plasma modulations is determined by the SLM pattern, the beam magnification between the SLM and the axicon, and the axicon base angle. The refractive axicons used in these experiments generate a one-to-one mapping of the beam power in an annulus at radius r and thickness dr to the power in an axial line element at position z and thickness dz [24]. This effectively yields a magnification factor of the radial modulations dependent on the axicon base angle given by

$$S = \frac{dz}{dr} = \frac{1}{\tan\gamma} - \tan\alpha, \quad (5)$$

where $\gamma = \sin^{-1}(n\sin\alpha) - \alpha$ is the approach angle of refracted rays toward the axis, n is the axicon refractive index, and α is the axicon base angle. The following experiments utilized an SLM with 20 μm pixels magnified by a factor of 2 onto a 28° base angle fused silica axicon, yielding a minimum modulation period of the line focus intensity of ~260 μm.

The setup illustrated in Fig. 1 uses a 1064 nm, 140 ps long Nd:YAG laser pulse, which is split into high- and low-power pulses. The low-power pulse reflects off the SLM (Hamamatsu LCOS-SLM, nematic liquid crystal on silicon) with 95% efficiency, picking up a programmable phase shift profile. The low- and high-energy pulses are then recombined at a nonpolarizing beam splitter and imaged through an axicon to the line focus, generating an axially modulated plasma waveguide. A synchronous 1064 nm, 140 ps probe pulse split from the main beam

passes through the plasma and is imaged into a folded wavefront interferometer to produce interferograms or shadowgrams. The interferograms are processed using a fast Fourier transform technique to extract the phase shift on the probe [25]. Resulting phase shift images are then low-pass-filtered to reduce noise and Abel-inverted to extract the 2D (axial and radial) electron density profile.

In initial experiments, modulated plasmas generated in air were probed at 2 ns delay. First, 130 mJ and 10 mJ were used in the high- and low-power arms, respectively. In this configuration, the minima of the modulated Bessel beam were below the breakdown threshold of air, allowing non-ionized sections. Figure 2 shows shadowgrams for a plasma generated using a phase pattern of equally spaced thin concentric rings imposed on the SLM arm [Fig. 2(a)]. This leads to a heater profile with concentric thin annular minima, which map to non-ionized regions notched in the plasma with a 400 μm modulation period [Fig. 2(b)]. Such a structure is of interest for guided, quasi-phase-matched high harmonic generation, with harmonics generated primarily in the notched zones. The conjugate pattern shows a series of separated plasma lenslets where the notches were formerly located [Fig. 2(d)]. Without the SLM, the plasma is uniform [Fig. 2(c)].

Quasi-phase matching of both direct laser acceleration [11] and laser wakefield acceleration [21] would benefit from a modulated plasma waveguide without neutral sections. To demonstrate the technique's utility for quasi-phase-matched acceleration experiments, the radially modulated beam was directed into a vacuum chamber and focused by a 28° axicon to overfill a 7 mm long cryogenically cooled nitrogen cluster jet [16–19] operated in pulsed mode. The peak intensity of the Bessel beam was located ~1 cm above the jet orifice. Axially modulated waveguides were formed using 450 mJ in the high-power arm and 10 mJ in the low-power arm (a ~2% contribution), giving an intensity modulation depth at the target of ~30%.

Abel-inverted electron density profiles of a 2.5 mm section of the 7 mm long modulated waveguide probed 1 ns after breakdown are shown in Fig. 3. Figure 3(a) shows the channel profile with the SLM arm blocked, yielding a straight channel with no periodic modulations. Figure 3(b) shows a modulated

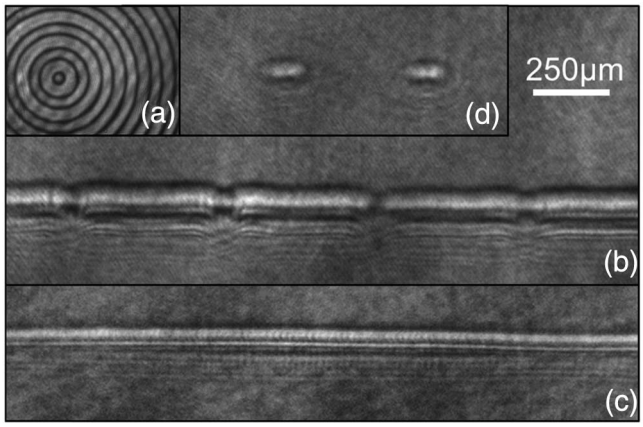

Fig. 2. (a) Image of a ~150 mJ, 140 ps laser pulse with notched minima, and (b) the corresponding plasma with notched non-ionized regions. (c) Without the SLM patterning, the resulting plasma is uniform. (d) Plasma generated with phase pattern conjugate to (b): isolated plasma lenslets are now where the notches were.

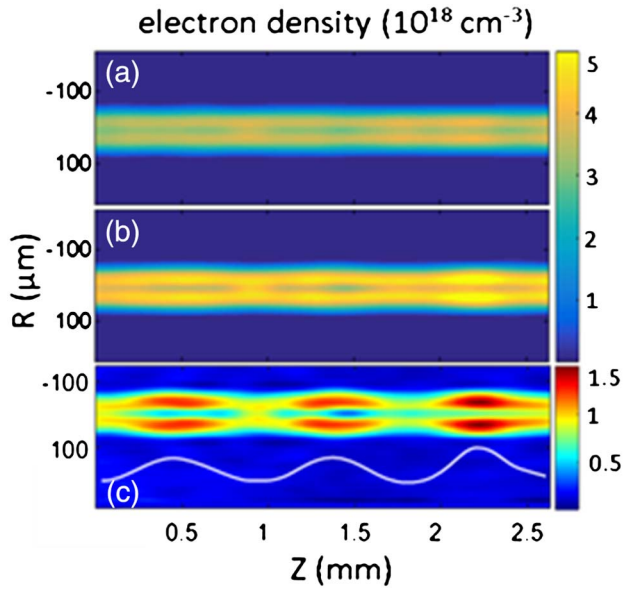

Fig. 3. Electron density of plasma waveguides in N_2 clusters formed with and without modulations. (a) An unmodulated plasma waveguide formed using only the high-power arm. (b) A plasma waveguide with an 860 μm period. (c) Difference between modulated and unmodulated densities, with the white curve showing the radially averaged difference. The color bars are in units of 10^{18} cm^{-3}.

channel formed by applying an SLM phase pattern with a 6 pixel radial modulation period. Finally, for clarity, the difference between Figs. 3(a) and 3(b) is shown in Fig. 3(c) to highlight the axial modulations of ~860 μm period imposed by the addition of the phase-modulated beam, giving a ~10% modulation in the peak density at the waveguide wall. In prior work with cluster jet waveguides, we have measured the lowest order mode propagation of injected pulses, with energy throughputs in the range of 10%–80%, depending on the details of jet parameters and axial modulations [16–19].

We note that use of clustered gas jets makes possible access to average electron densities over the range of ~10^{15}–10^{22} cm^{-3}, which is a huge span enabling high harmonic generation [1] and laser wakefield acceleration [26] in multiple density regimes and with a wide range of possible laser wavelengths. This is because laser heating and ionization are very efficient on an individual cluster basis [16–19], while average electron density can be controlled by the initial number of clusters per unit volume.

In summary, we have demonstrated the SLM-based patterning of intense laser pulses in an interferometric configuration that reduces the required laser fluence on the SLM. These intense patterned pulses can be used to create axially modulated plasma waveguides in air and in cluster jets. Even with only ~2% of the laser energy in the SLM arm, the resulting plasma waveguide shows significantly modulated electron density. This technique allows a great deal of freedom for tuning the plasma structures for quasi-phase matching nonlinear optical processes and electron acceleration.

Funding. Defense Threat Reduction Agency (DTRA) (HDTRA11010045); U.S. Department of Energy (DOE) (DESC0007970); National Science Foundation (NSF) (PHY1301948).

REFERENCES

1. T. Popmintchev, M.-C. Chen, D. Popmintchev, P. Arpin, S. Brown, S. Alisauskas, G. Andriukaitis, T. Balciunas, O. D. Mücke, A. Pugzlys, A. Baltuska, B. Shim, S. E. Schrauth, A. Gaeta, C. Hernández-García, L. Plaja, A. Becker, A. Jaron-Becker, M. M. Murnane, and H. C. Kapteyn, Science **336**, 1287 (2012).
2. L. Bergé, S. Skupin, and G. Steinmeyer, Phys. Rev. A **79**, 033838 (2009).
3. A. Couairon, J. Biegert, C. P. Hauri, W. Kornelis, F. W. Helbing, U. Keller, and A. Mysyrowicz, J. Mod. Opt. **53**, 75 (2006).
4. V. M. Malkin, G. Shvets, and N. J. Fisch, Phys. Plasmas **7**, 2232 (2000).
5. W. Cheng, Y. Avitzour, Y. Ping, S. Suckewer, N. J. Fisch, M. S. Hur, and J. S. Wurtele, Phys. Rev. Lett. **94**, 045003 (2005).
6. T. M. Antonsen, J. P. Palastro, and H. M. Milchberg, Phys. Plasmas **14**, 033107 (2007).
7. K. Y. Kim, A. J. Taylor, J. H. Glownia, and G. Rodriguez, Nat. Photonics **2**, 605 (2008).
8. J.-C. Diels, R. Bernstein, K. E. Stahlkopf, and X. M. Zhao, Sci. Am. **277**, 50 (1997).
9. M. Clerici, Y. Hu, P. Lassonde, C. Milian, A. Couairon, D. N. Christodoulides, Z. Chen, L. Razzari, F. Vidal, F. Legare, D. Faccio, and R. Morandotti, Sci. Adv. **1**, e1400111 (2015).
10. T. Tajima and J. M. Dawson, Phys. Rev. Lett. **43**, 267 (1979).
11. A. G. York, H. M. Milchberg, J. P. Palastro, and T. M. Antonsen, Phys. Rev. Lett. **100**, 195001 (2008).
12. D. J. Spence and S. M. Hooker, Phys. Rev. E **63**, 015401 (2000).
13. C. G. Durfee and H. M. Milchberg, Phys. Rev. Lett. **71**, 2409 (1993).
14. D. Kaganovich, P. V. Sasorov, Y. Ehrlich, C. Cohen, and A. Zigler, Appl. Phys. Lett. **71**, 2925 (1997).
15. C. G. R. Geddes, C. Toth, J. van Tilborg, E. Esarey, C. B. Schroeder, D. Bruhwiler, C. Nieter, J. Cary, and W. P. Leemans, Nature **431**, 538 (2004).
16. A. J. Goers, S. J. Yoon, J. A. Elle, G. A. Hine, and H. M. Milchberg, Appl. Phys. Lett. **104**, 214105 (2014).
17. B. D. Layer, A. G. York, T. M. Antonsen, S. Varma, Y.-H. Chen, Y. Leng, and H. M. Milchberg, Phys. Rev. Lett. **99**, 035001 (2007).
18. H. M. Milchberg, K. Y. Kim, V. Kumarappan, B. D. Layer, and H. Sheng, Philos. Trans. R. Soc. London, Ser. A **364**, 647 (2006).
19. H. Sheng, K. Y. Kim, V. Kumarappan, B. D. Layer, and H. M. Milchberg, Phys. Rev. E **72**, 036411 (2005).
20. G. A. Magel, M. M. Fejer, and R. L. Byer, Appl. Phys. Lett. **56**, 108 (1990).
21. S. J. Yoon, J. P. Palastro, and H. M. Milchberg, Phys. Rev. Lett. **112**, 134803 (2014).
22. S. J. Yoon, A. J. Goers, G. A. Hine, J. D. Magill, J. A. Elle, Y.-H. Chen, and H. M. Milchberg, Opt. Express **21**, 15878 (2013).
23. M.-W. Lin, Y.-M. Chen, C.-H. Pai, C.-C. Kuo, K.-H. Lee, J. Wang, S.-Y. Chen, and J.-Y. Lin, Phys. Plasmas **13**, 110701 (2006).
24. J. Sochacki, A. Kołodziejczyk, Z. Jaroszewicz, and S. Bará, Appl. Opt. **31**, 5326 (1992).
25. M. Takeda, H. Ina, and S. Kobayashi, J. Opt. Soc. Am. **72**, 156 (1982).
26. A. J. Goers, G. A. Hine, L. Feder, B. Miao, F. Salehi, J. K. Wahlstrand, and H. M. Milchberg, Phys. Rev. Lett. **115**, 194802 (2015).